



## Research paper

## Combining microwave resonance technology to multivariate data analysis as a novel PAT tool to improve process understanding in fluid bed granulation

Vera Lourenço<sup>a,b</sup>, Thorsten Herdling<sup>b</sup>, Gabriele Reich<sup>c</sup>, José C. Menezes<sup>a</sup>, Dirk Lochmann<sup>b,\*</sup><sup>a</sup> Institute of Biotechnology and Bioengineering, IST, Technical University of Lisbon, Portugal<sup>b</sup> Quality Operations, PAT – Laboratory, Merck Serono, Darmstadt, Germany<sup>c</sup> Department of Pharmaceutical Technology and Biopharmaceutics, University of Heidelberg, Germany

## ARTICLE INFO

## Article history:

Received 8 September 2010

Accepted in revised form 12 February 2011

Available online 17 February 2011

## Keywords:

Fluid bed granulation

PAT

Microwave resonance technology

Multivariate data analysis

Batch monitoring

QbD

## ABSTRACT

A set of 192 fluid bed granulation batches at industrial scale were *in-line* monitored using microwave resonance technology (MRT) to determine moisture, temperature and density of the granules. Multivariate data analysis techniques such as multiway partial least squares (PLS), multiway principal component analysis (PCA) and multivariate batch control charts were applied onto collected batch data sets. The combination of all these techniques, along with *off-line* particle size measurements, led to significantly increased process understanding. A seasonality effect could be put into evidence that impacted further processing through its influence on the final granule size. Moreover, it was demonstrated by means of a PLS that a relation between the particle size and the MRT measurements can be quantitatively defined, highlighting a potential ability of the MRT sensor to predict information about the final granule size.

This study has contributed to improve a fluid bed granulation process, and the process knowledge obtained shows that the product quality can be built in process design, following *Quality by Design* (QbD) and *Process Analytical Technology* (PAT) principles.

© 2011 Published by Elsevier B.V.

## 1. Introduction

Granulation is a unit operation used in pharmaceutical industries for decades to convert fine powders into larger granules, which are (1) safer to manipulate, have (2) improved flow properties and (3) better compression properties, compared to powders [1]. Fluid bed dryers are commonly used to perform wet granulation and subsequent drying. In wet granulation processes, the granule moisture is a very important critical quality attribute (CQA) [2], as several granule properties depend on it, e.g. chemical stability, hardness and flowability. The classical approach to detect granulation end-points is based on outlet air temperature or product temperature [3] and in practice is determined by collecting samples and measuring the granule moisture *at-line*, until the target moisture value is achieved. This way of end-point determination is time-consuming and often leads to reworks, whenever the target residual moisture content of the granules is overshoot.

So far, the most common analytical technology for continuous moisture determination is near-infrared (NIR) spectroscopy, and several attempts to monitor fluid bed granulations have already

been made [4–6]. Nevertheless, there are some drawbacks in NIR monitoring: (a) short radiation penetration in the solid bed, which enables only the determination of surface moisture, (b) measurements are affected by the material density [7] and (c) fouling of the optical sensor window.

More recently, a new technology for monitoring granule moisture emerged, which is the microwave resonance technology (MRT). This technique captures the interaction between water molecules and changing electromagnetic fields. The derived MRT signal is a band whose frequency peak and bandwidth decrease with increasing water and material load, allowing therefore a simultaneously independent measurement of moisture and density of the solid products. This signal is dependent on the absolute temperature of the material; therefore, a thermocouple is usually incorporated together with the resonance sensor. A more detailed explanation can be found elsewhere in the literature [8–10]. The microwave resonance technology has been already used to measure moisture *in-line* in various industrial processes, such as in food [11,12], paper [13] and agro [14] industries. Likewise, attempts to monitor moisture *in-line* in pharmaceutical granulation have been successfully made [2,15], although at small scale. It was shown that the MRT sensor was able to determine the particles moisture during a fluid bed drying, with precision and accuracy, being equivalent to the *at-line*

\* Corresponding author. Tel.: +49 6151 728569; fax: +49 6151 723150.

E-mail address: [dirk.lochmann@merck.de](mailto:dirk.lochmann@merck.de) (D. Lochmann).

loss on drying using infrared light (LOD/IR) and *off-line* Karl-Fischer titration methodologies [2]. Moreover, because sample withdrawing and analysis were not required, a 75% of time saving during the drying phase could be achieved [2].

Although MRT has been used only to monitor the solid bed moisture and determine the granulation end-point in pharmaceutical processes, much more can be done with this technology. Besides moisture, also density and temperature are measured at high frequency. Therefore, a significant amount of information can be generated with just a few batches, reproducing the trajectories of those variables, which can then be used to study and compare different batches. Even if there are only three parameters, the high sampling frequency and the accuracy of measurements make it ideal for use of multivariate data analysis (MVDA) techniques in order to extract information from the large data set and gain knowledge on multiple process batches, covering or including several sources of nominal process variability. MVDA makes possible to see how the variables are correlated to each other and what the signature represented by batch trajectories is. In that way, it is possible to distinguish “successful” batches from “unsuccessful” batches. Furthermore, early in the process, it is possible to predict whether a batch will end at the desired end-point (state) and how long it will take, based on the established average profile, allowing earlier fault diagnosis to be made and possible corrective actions to be taken prior to discharge. Some common MVDA techniques used for batch monitoring are multiway PCA, multiway PLS and multivariate control charts [16]. In the literature information about MVDA techniques, their fundamentals, applications and interpretability can be found [16–19]. The combination of *in-line* MRT monitoring and MVDA is therefore a novel and powerful tool leading to improved process understanding. Product quality is a multivariate set of properties or univariate specifications that many times are correlated. Moreover, product quality depends on the whole process trajectory (set of processing events or path) and not only on the end-point [16]. Granule growth is a complex process. During this process, the granule properties such as moisture change. Therefore, a batch trajectory or process history will have a strong influence on the final product quality, concerning the granule properties. The moisture content is a well-known CQA, as already mentioned, but some other are recommended to be taken as well as potential critical attributes, such as homogeneity, mechanical strength, shape, flowability and bulk/tapped density [20]. All these properties can affect subsequent processing steps, such as blending and tableting [1]; ultimately, granule characteristics can even affect the dissolution profiles and therefore the bioavailability of the final drug product in a patient [21], thus the reason to define such properties as CQAs.

The use of MVDA combined with *in-line* monitoring techniques conforms to the US Food and Drug Administration (FDA) PAT initiative and the QbD concept, published in the 2004 FDA guidance [22] and later in ICH guidelines [23,24]. The PAT initiative emphasises the need to understand all critical sources of variability affecting a pharmaceutical process to ensure that good-quality drug products are consistently obtained. To achieve this goal, existing guidance recommends the use of process analysers that can provide timely and non-destructive measurements, multivariate tools for design, data acquisition and analysis, process control tools, continuous improvement and knowledge management tools. Moreover, in an integrated perspective, chemical, physical, microbiological, mathematical and risk analysis tools should be included [22].

In this study, we report the gained process knowledge through the use of a real-time process analyser based on MRT, combined with MVDA techniques, applied to an industrial fluid bed granulation and drying steps of a pharmaceutical product. Useful information was obtained and used to improve the process, following the path to *Quality by Design*.

## 2. Materials and methods

### 2.1. Materials

The powder mixture consisted of one API and two excipients. The binder was provided as an aqueous solution. All the raw materials were obtained from approved suppliers and conformed to European and US Pharmacopoeias. The total mass of each batch was more than 500 kg (industrial scale).

### 2.2. Microwave resonance technology

The microwave resonance technology Hydorpharm fbma and the software MWF-Standard were both supplied by Döschner & Döschner GmbH (Hamburg, Germany). The sensor was assembled onto the fluid bed dryer according to the cGMP for new equipment qualification, calibration and validation. Each 20 s, the averages of the acquired values for temperature, density and moisture were stored. The calibration of the sensor was performed by taking samples from the fluid bed dryer and analysing them by LOD/IR and Karl-Fischer titration. A good agreement between the moisture values obtained from the MRT and the reference methods was always found ( $R^2 > 0.95$ ) within the moisture range from 1% to 12%. The maximum moisture content achieved during this study was below 10%. The established calibration equation was periodically monitored during the time of this study. The technical details of the system can be found elsewhere [25].

### 2.3. Particle size characterisation

The particle size distribution of final product samples from 34 selected granulation batches was analysed using an *off-line* particle sizing system (Mastersizer 2000, Malvern Instruments, Worcestershire, UK). The samples were air dispersed (0.5 bar) using a dry powder feeder module (Scirocco 2000, Malvern Instruments, Worcestershire, UK).

### 2.4. Granulation set-up

All granulations were performed in a full-scale routine WSG200 fluid bed dryer (Glatt GmbH, Binzen, Germany). In the same vessel, granulations and subsequent drying steps were carried out. All the process parameters were set as nominal.

### 2.5. Multivariate data analysis software

The multivariate data analysis was performed using SIMCA-P+ 12.0 (Umetrics, Umeå, Sweden). The interval PLS (iPLS) algorithm was performed using Matlab R2007b v.7.5 (Mathworks, Inc., USA) with PLS toolbox v.4.0 (Eigenvector Research Inc., USA).

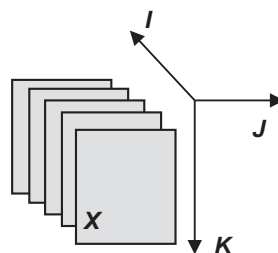
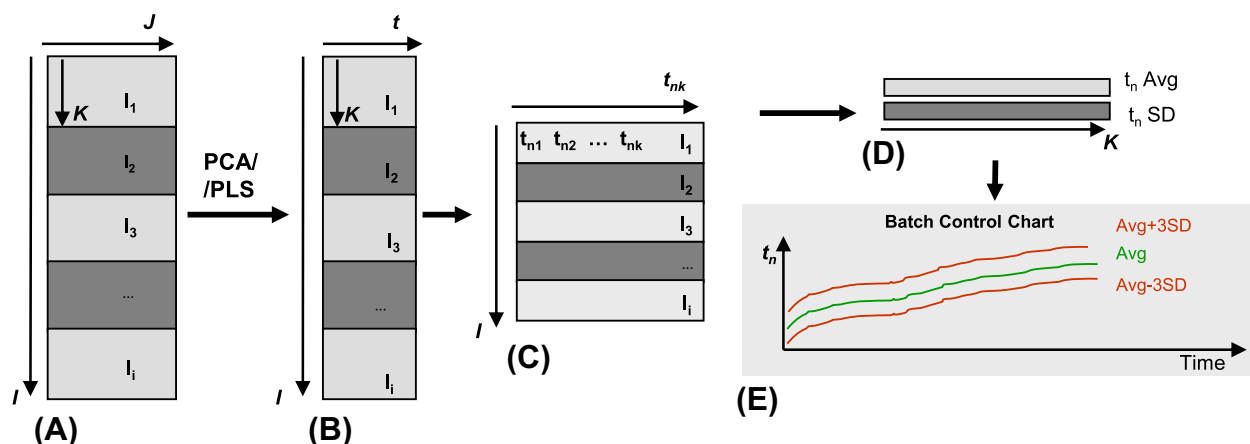
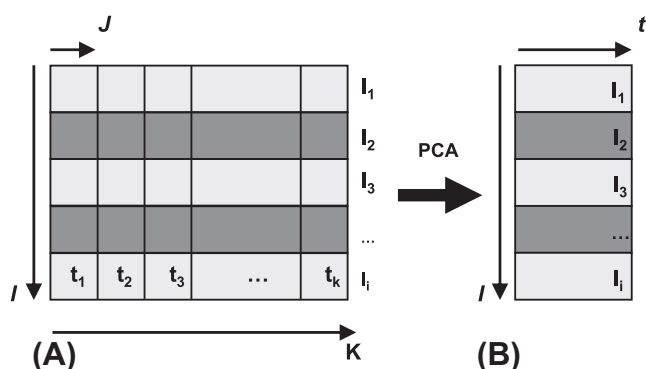


Fig. 1. Three-dimensional nature of process data: for each batch *I*, matrix *X* is composed by *J* variables measured at *K* time intervals.



**Fig. 2.** Variablewise unfolding and batch control charts limits. The batches are arranged on top of each other (A); then, a PCA or PLS can be applied, and scores ( $t$ ) are generated (B). For each principal component/latent variable  $t_n$  (C), the average and standard deviation of the batches scores for each sampling time are calculated (D) and plotted against time (E). (For interpretation of the references to colour in this figure legend, the reader is referred to the web version of the article.)



**Fig. 3.** Batchwise unfolding: each row consists of a whole batch, where the columns are time ordered and contain the several variables measured at each time (A). After applying a PCA, scores are generated, and each score will represent a whole batch (B).

## 2.6. Data and pre-processing

The data set for this study consisted of 192 granulation batches, produced from January until July of a particular year. Three vari-

ables were monitored by the MRT sensor covering the whole duration of the batches: moisture, temperature and density of the particles. To enhance the signal to noise ratio, a Savitsky–Golay smoothing filter [26] was used for moisture and density (21-points window and a first-order polynomial).

Each run had a different duration. Thus, batch alignment or synchronisation of process trajectories had to be performed. The objective was to establish common starting points at different phases of the run and to match the shape of the trajectories of the variables [18]. Because there are three different stages during a granulation batch (viz, mixing, spraying and drying phases), the transition points between two consecutive phases were used to do the synchronisation. Then, within each phase, the batches may still not have the same length, but the shape of the trajectories will match each other more closely. The methodology used to align trajectories was dynamic time warping. This technique translates, expands and contracts localised segments within two trajectories to achieve a minimum distance between them [27]. That algorithm was used as implemented in the software where the data analysis was performed. Finally, the data was centred and scaled to unit variance to assure that all three variables spanned the same range.

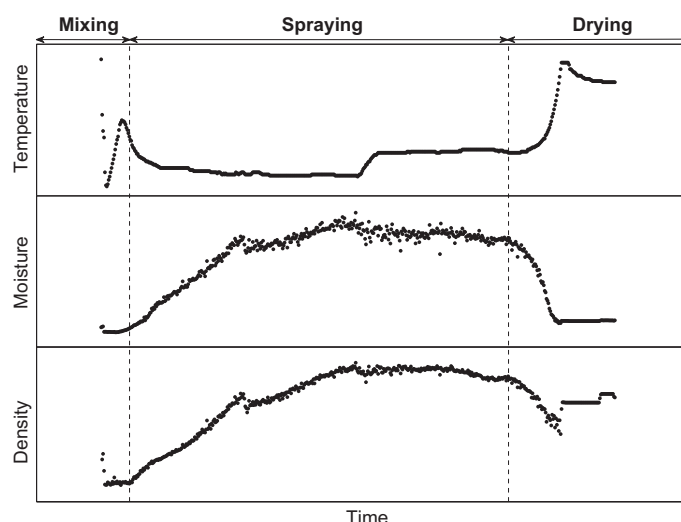


**Fig. 4.** Typical time profiles for granule temperature, moisture and density during a granulation. The dashed lines show the separation between the phases of mixing, spraying and drying.

**Table 1**  
Multiway PLS model indicators. Number of principal components (PC),  $R^2_X$  (the variance of the three variables explained by the model),  $R^2_Y$  (the variance of the time dependency explained by the model) and  $Q^2$  (the fraction of total variance of the time that can be predicted by the model, as estimated by the cross-validation).  $Q^2 = (1 - \text{PRESS}/\text{SS})$ , where PRESS is the prediction error sum of squares, and SS is the residual sum of squares.

	Data set A (192 batches)			Data set B (129 batches)		
	Mixing	Spraying	Drying	Mixing	Spraying	Drying
PC	2	2	2	2	2	2
$R^2_X$	0.659	0.772	0.835	0.639	0.676	0.948
$R^2_Y$	0.010	0.632	0.164	0.126	0.750	0.463
$Q^2$	0.010	0.632	0.163	0.126	0.750	0.463

2.7. Multivariate process analysis

The methodology used for batch process analysis is described in the literature [18]. In summary, there are two main steps. First, historical data are used to model the process. Atypical (non-nominal) trajectories or different batch clusters are identified; contribution

plots are a helpful tool in diagnosing the probable causes for the major differences among differing batches. Second, the typical or nominal batches are selected, and a model is built using their data alone. With that new model, control charts can be calculated and used later to monitor future batches.

2.7.1. Observation-level modelling and batch control charts

When  $J$  process variables are measured at  $K$  time intervals, for each one of  $I$  batches, the whole data set can be assumed as a three-dimensional data array  $X (J \times K \times I)$  (Fig. 1). One way of unfolding the 3D matrix into 2D is arranging the batches one on top of each other. Each column will represent one variable, and each row will correspond to a certain sampling time of a given batch (Fig. 2A). Then, common multivariate analysis tools such as PCA or PLS can be applied to the resulting 2D data matrix.

With the generated scores from the PCA or PLS techniques, it is possible to compute the control limits for the process very easily. For each sampling time, the average and standard deviation of the scores of all batches are computed and plotted *versus* time (Fig. 2B–E).

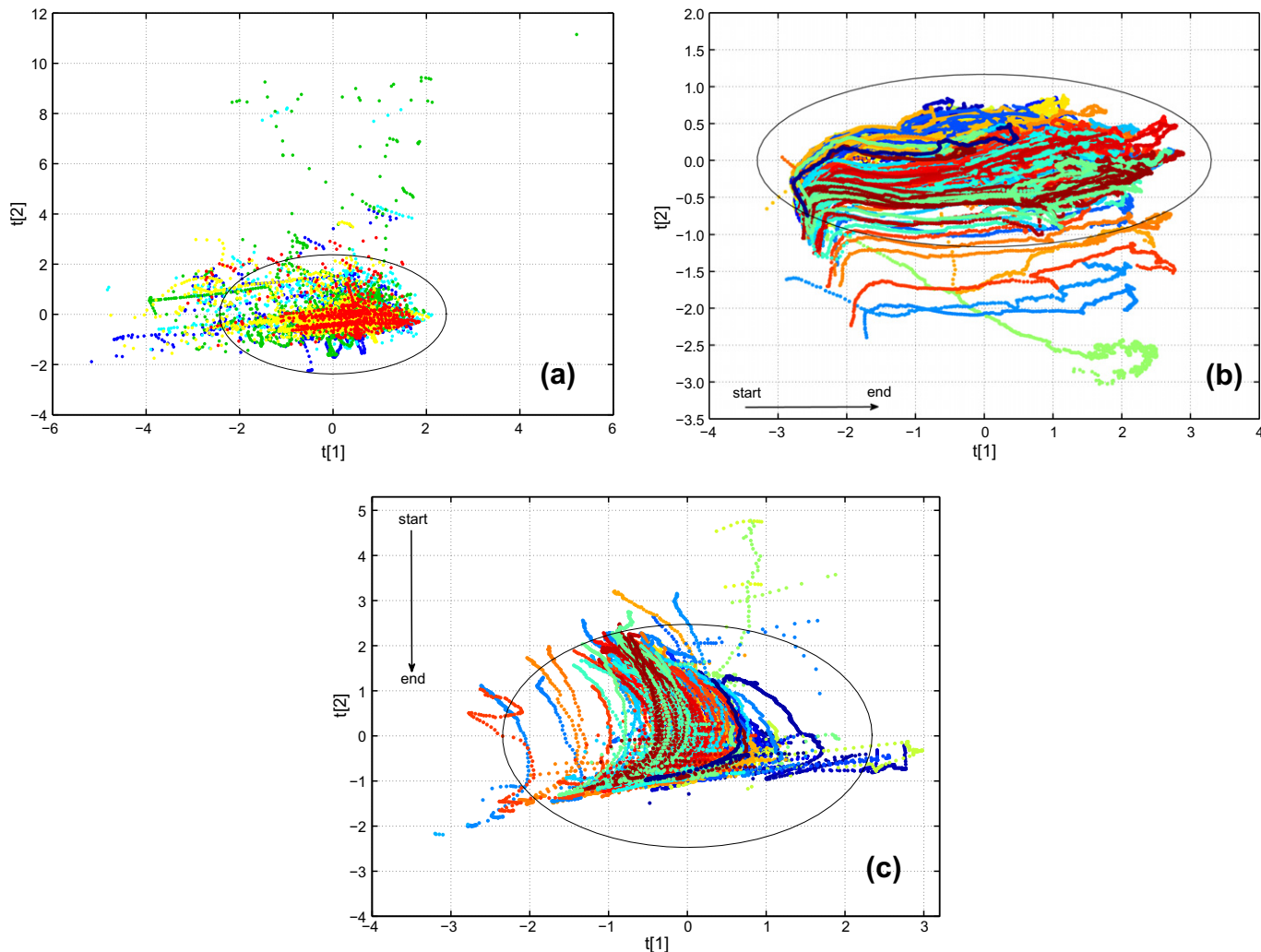


**Fig. 5.** Score plots for the different phases of the process: (a) mixing, (b) spraying and (c) drying. In the mixing phase plot (a), the scores are coloured according to batch maturity (batch starts in blue, evolves to green and ends in red); the majority of the scores at the end of the mixing phase are inside the Hotelling's  $T^2$  limits. In the spraying (b) and drying (c) phases, the scores are coloured according to the batches. (For interpretation of the references to colour in this figure legend, the reader is referred to the web version of the article.)

### 2.7.2. Batch-level modelling

A 3D matrix can also be unfolded in a different way; each row corresponds to a whole batch, and the columns are the variables measured for all the sampling times (Fig. 3). This batchwise or batch-level unfolding will allow comparing the batches as a whole, eliminating the time dependency of the trajectories. Instead of the variables on the columns, the scores from a previous observation-level PCA can also be used, reducing the calculation times. The scores that are generated from the batch-level model can be later correlated to quality attributes of raw materials or intermediate/final products through PLS models.

The type of unfolding should be selected depending on how similar batches are to each other. The observation level is used when batches are production batches (reasonably similar to each other), whereas batch-level unfolding is used especially in designed experiments or with non-nominal batches.

### 2.8. Correlation between particle size and MRT monitoring

To check whether there was any correlation between process path (given by the timely MRT monitoring) and final quality of the product (viz, granule particle size distributions), a PLS model was developed. As X-data set, the particle size distributions of the final granules were used (particle size ranged from  $10^{-2}$   $\mu\text{m}$  until  $10^4$   $\mu\text{m}$ ) after mean centring; the Y-data set consisted of the first principal component scores of the batch-level model (built upon the MRT measurements for the whole historical data set). To improve the prediction ability of the PLS model, a variable selection algorithm was used, *i*PLS [28]. This algorithm develops local PLS models on equidistant subintervals of the variable full range; the prediction performance of these local PLS models is then compared to the PLS model using the full range, based on the root mean square error of cross-validation (RMSECV) or on the root mean

square error of prediction (RMSEP) for an external data set, defined, respectively, as:

$$\text{RMSECV} = \sqrt{\frac{\sum_{i=1}^n (Y_{i(\text{CV})} - Y_{i(\text{exp})})^2}{n}} \quad (1)$$

$$\text{RMSEP} = \sqrt{\frac{\sum_{i=1}^n (Y_{i(\text{pred})} - Y_{i(\text{exp})})^2}{n}} \quad (2)$$

where  $n$  stands for the number of prediction samples,  $Y_{i(\text{CV})}$  and  $Y_{i(\text{pred})}$  for predicted values for cross-validation and external validation, respectively, and  $Y_{i(\text{exp})}$  for the experimental values of sample  $i$ .

## 3. Results and discussion

### 3.1. Historical data analysis

As mentioned earlier, it is useful to start with a preliminary analysis of all available historical batches. Therefore, all 192 routine batches were considered. All were batches *within-specification* according to the existing criteria at the plant. Each batch was divided into the three main phases: mixing, spraying and drying (Fig. 4). This made it easier to align the batches. Then, for each phase, an independent PLS model *versus* time was developed (Table 1). Moreover, because each phase has different characteristics, different phenomena occurring with different kinetics, applying linear techniques such as PCA or PLS to the whole process would not produce results as good as splitting the process into phases where similar phenomena dominate.

The score plot for the mixing phase shows that there is no common trajectory (Fig. 5a). This is a period when all the powders are mixed until homogeneity is achieved. For almost all batches, the mixing phase ends in a common region inside the Hotelling's  $T^2$  el-

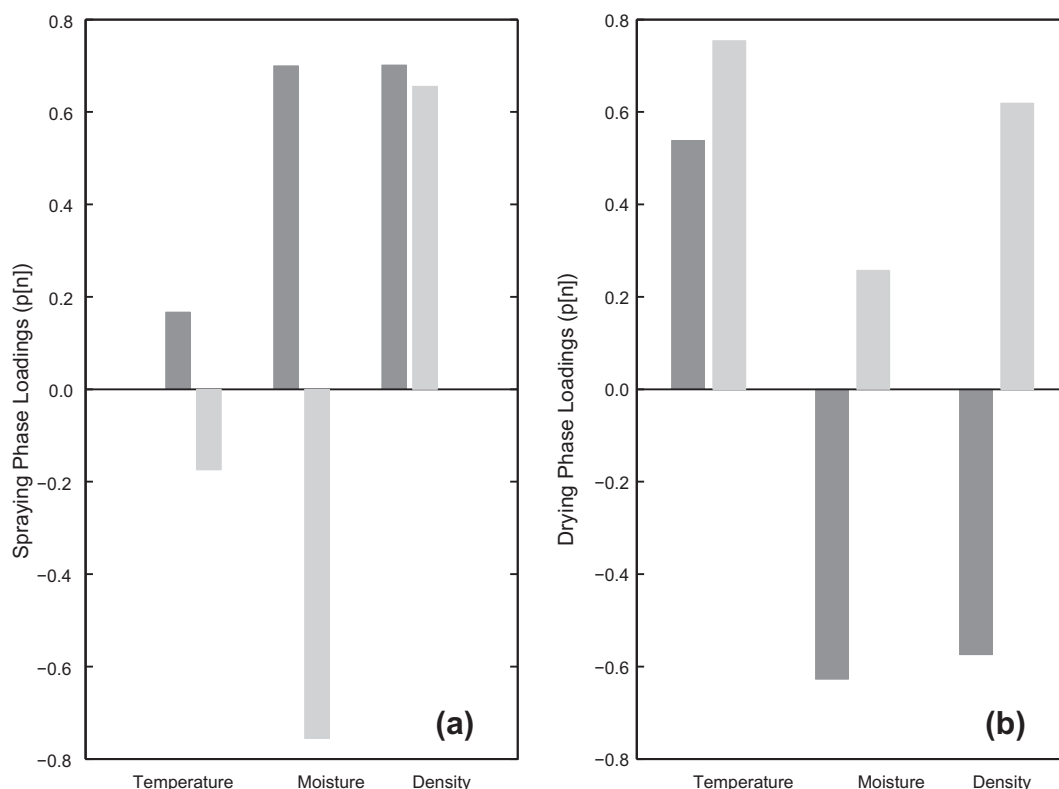


**Fig. 6.** Loading plots for spraying (a) and drying (b) phases. The dark columns refer to the first principal component of the models, whereas the light columns refer to the second principal component.



lipse. The score plots for the spraying and the drying phases do show a common trajectory, a process signature for each phase (Fig. 5b–c). In the spraying phase, the initial scores are on the left region of the ellipse, and the process evolves along the first principal component axis; the final scores are nearly all within the confidence limits. In the drying phase, the process evolves from the upper part of the chart to the bottom, along the opposite direction of the second principal component axis. As previously mentioned, also almost all final scores are within the Hotelling's  $T^2$  limits.

Looking at the loading plot of the spraying and drying phases (the mixing phase is not important because there is no common trajectory the batches should follow), all three variables are correlated (Fig. 6). There is a thermodynamic relation between temperature and moisture [3,29], and density also depends partially on the water content of the solids. For the spraying phase, both principal components are dominated by moisture and density, although in different ratios; for the drying phase, all the variables play an important role for both principal components. In those two phases, some batches are outside the Hotelling's  $T^2$  confidence limits but show the same common trajectory shape. That indicates a process drift along time and the contribution of different variables. For instance, in the spraying phase, the batches lying outside

the ellipse show a drift compared to the ones inside, because they have lower second principal component scores. In terms of original variables, all these batches presented temperature and moisture profiles higher than the average values. However, because PLS models extract the most important sources of variation within a data set, there is an increased sensitivity towards what is not typical for that given data set (i.e. for what is not common across most batches). In this study, only the information provided by the *in-line* microwave sensor was considered; the use of other information such as process parameters was beyond the scope of this study.

### 3.2. Batch modelling

#### 3.2.1. Observation-level modelling and multivariate batch control charts

The exploratory analysis performed earlier has included all the historical data (Data set A, Table 1). For purposes of batch modelling and calculation of batch control charts limits, only the typical trajectories were considered (Data set B, Table 1). All batches that presented some kind of deviation or drift compared to the majority were discarded, i.e. the batches whose scores lay systematically outside the ellipse for the spraying phase (Fig. 5b) as well as the

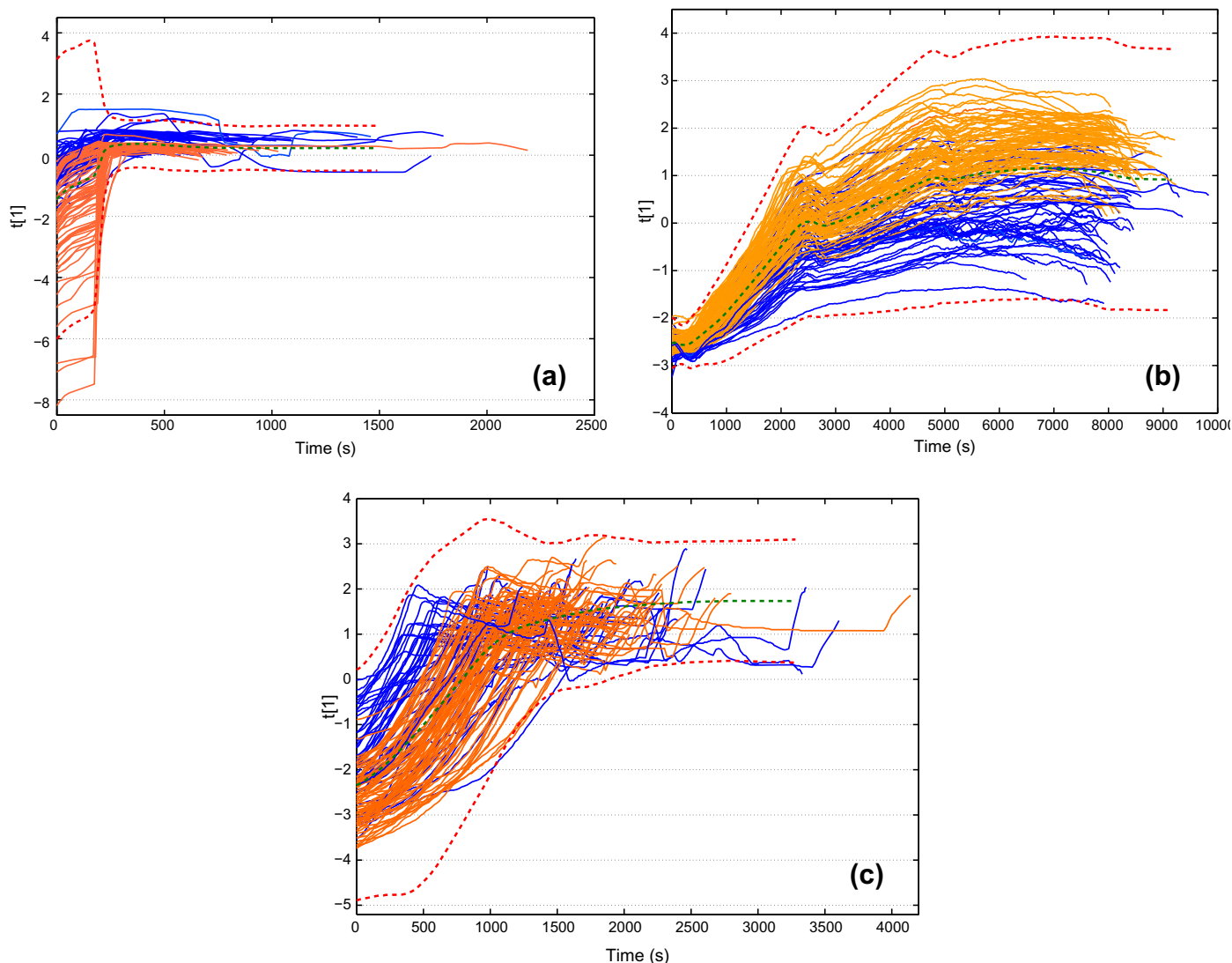


**Fig. 7.** Multivariate batch control charts for each granulation phase: (a) mixing, (b) spraying and (c) drying. Batches are coloured according to production month (January–March: blue, April–July: orange). (For interpretation of the references to colour in this figure legend, the reader is referred to the web version of the article.)

batches whose drying time exceeded 50% of the average time. Then, new PLS models were generated for each process phase.

In Fig. 7, the multivariate batch control charts generated with the first principal component scores of each PLS model are shown. During the mixing phase, a large variability can be seen at the beginning of the process, and then, all the batches converge to a steady stage, which can be attributed to the homogeneity of the powder mixture. As the spraying phase proceeds, the variability of the process starts to increase. The control limits are wider at the end of this phase, although the main process parameters are controlled (inlet air temperature, inlet air flow rate and binder spraying rate). During the drying phase, samples are withdrawn and analysed *at-line* by LOD/IR. In this control chart, it can also be seen that there is a set of batches that present a time shift on the profile when compared to the remaining, i.e. there is a set of batches that show the inflection point that could correspond to the change of water evaporation kinetics earlier in the drying [30]. Those heterogeneities make the duration of the drying phase variable and harder to establish narrow control limits; however, the variability is larger at the beginning than at the end of this phase, because at the end, a moisture target must be met. From the three control charts, something is evident: there is a trend on the first principal component scores that matches the season of the year (i.e. production months). Batches that were produced from January until March (colder months) form a cluster, and batches that were produced from April until July (warmer months) form another cluster. Going back to the original variables recorded by the microwave sensor, it is seen that the granule temperature, for example, shows the same trend: during the spraying, the particles show lower temperatures for colder months and higher temperatures for warmer months (Fig. 8). Since the process is run always at the same nominal conditions, namely for the inlet air temperature, this can be an evidence of the influence of the inlet air relative humidity. This is in agreement with the control chart for the drying phase in Fig. 7c, where it can be seen that the batches drying faster are the ones produced during cold months, when the inlet air has lower relative humidity. At this point, it is possible to attribute a root cause for the drift of some batches belonging to the historical data set, which were lying outside the ellipse (Fig. 5b). These batches were produced during the warmer

months, and probably, the relative humidity of the air on those days was particularly higher than usual.

The batch control charts using the second principal component scores do not add any further significant information and therefore are not shown here.

### 3.2.2. Batch-level modelling

The PLS models scores of each phase of the process were combined and unfolded batchwise; this was done independently for both data sets A and B. Then, a PCA model for each data set was developed to see how the batches would distribute in relation to each other (Table 2).

The score plot in Fig. 9a shows that there is some variability within the whole historical data. Besides, there are some batches lying outside the Hotelling's  $T^2$  limits. This can be due to some particular process condition that occurred during those particular batches, such as a high relative humidity of the inlet air.

By using only the typical batches (data set B), nearly all scores are within the Hotelling's  $T^2$  limits (Fig. 9b). Those scores also show a trend on the first principal component according to the season of the year, as previously found on the observation-level modelling: the colder months batches have higher scores and the warmer months have lower scores. This is essentially the same information that was previously shown by the batch control charts. The advantage of the batch-level model is that now the whole batch information is condensed into one single score, which can be related to other batch properties (raw materials, intermediate and final prod-

**Table 2**

Batch-level PCA model indicators. Number of principal components (PC),  $R_X^2$  (the variance of the X-data set explained by the model) and  $Q^2$  (the fraction of total variance of the X-data set that can be predicted by the model, as estimated by the cross-validation).  $Q^2 = (1 - \text{PRESS}/\text{SS})$ , where PRESS is the prediction error sum of squares, and SS is the residual sum of squares.

	Data set A (192 batches)	Data set B (129 batches)
PC	5	5
$R_X^2$	0.854	0.849
$Q^2$	0.788	0.827

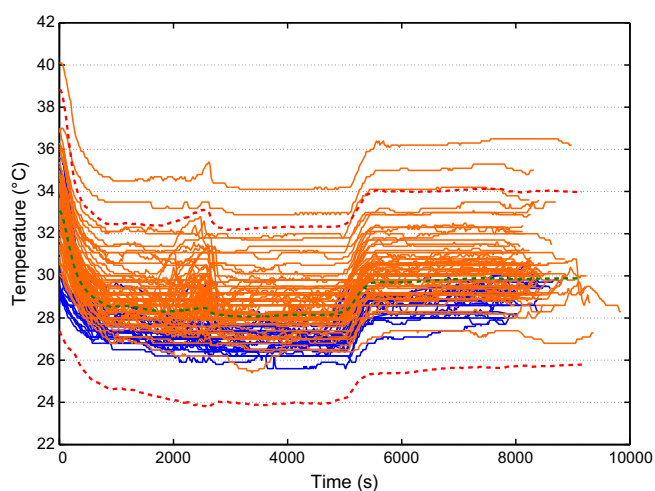


**Fig. 8.** Granule temperature profiles during spraying phase. Batches are coloured according to production month (January–March: blue, April–July: orange). Thick green dashed line: average temperature profile; thick red dashed lines: batch control chart limits for the granule temperature; solid lines: granule temperature profiles. (For interpretation of the references to colour in this figure legend, the reader is referred to the web version of the article.)

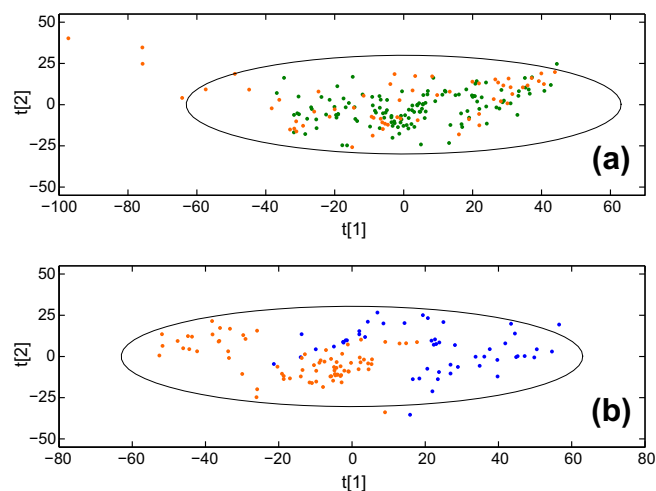


**Fig. 9.** Batch-level modelling: On the top (a), data set A was used. The orange dots correspond to the batches that were discarded for modelling purposes, and the green dots correspond to the batches belonging to data set B. On the bottom (b), data set B was used, and colours refer to production months (January–March: blue, April–July: orange). (For interpretation of the references to colour in this figure legend, the reader is referred to the web version of the article.)

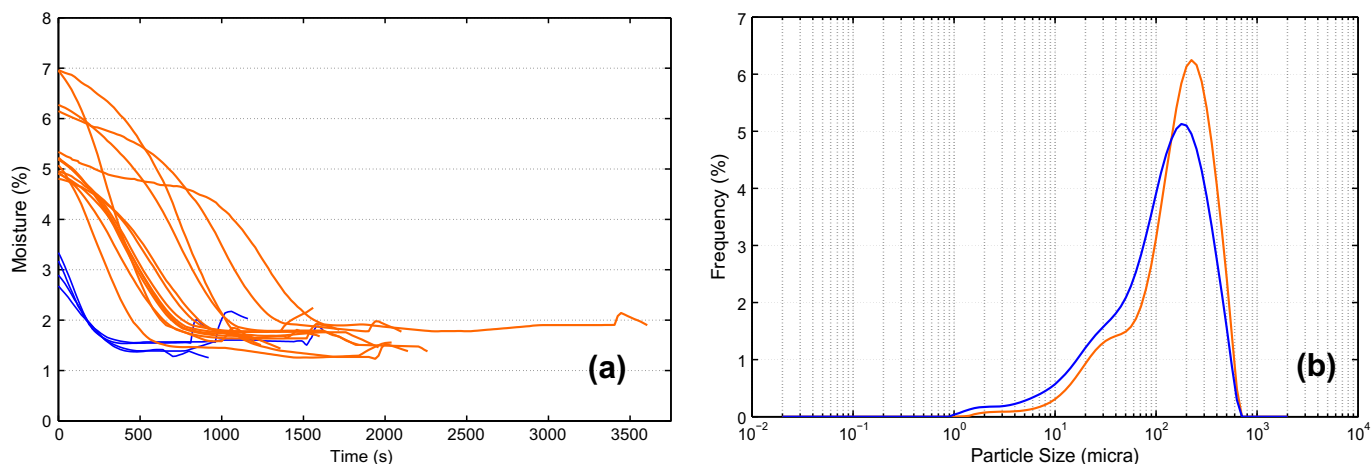


**Fig. 10.** Moisture profiles of granules during the drying phase (a); average particle size distributions of granules produced during different seasons of the year (b). Blue lines refer to batches produced during cold months (January–March), and orange lines refer to batches produced during warm months (April–July). (For interpretation of the references to colour in this figure legend, the reader is referred to the web version of the article.)

ucts properties and process parameters) that may not be directly time dependent.

### 3.3. Off-line particle size characterisation

The final granules of 34 batches within the historical data set were analysed for particle size properties. The selected samples were measured with a particle sizing system, and the particle size distributions (histograms) of the final granules were obtained.

The performed analysis showed that the granule size distribution on average was related to process trajectories followed for each particular batch. Granules produced during colder months had lower moisture content, dried faster, presented broader particle size distributions at the end of the process and had a higher proportion of fines. Conversely, granules that were produced during warmer months had higher moisture content, took longer to dry, presented at the end of the process narrower particle size distributions and had a smaller amount of fines (Fig. 10). The relation observed between granule moisture content during spraying and particle size distribution at the end is in agreement with other literature reports [31], where granules with higher moisture content during the granulation showed to be more resistant to breakage and attrition, originating less amount of fines and narrower particle size distributions, than lower moisture granules.

### 3.4. Correlation between particle size and MRT measurements

To quantify the observed relation between process trajectories (from MRT monitoring) and final granule particle distributions, a PLS model was developed using the iPLS methodology as a variable selection algorithm. This approach indicated the following particle size ranges as the best correlated to the batch-level model scores: from 12.6  $\mu\text{m}$  until 20  $\mu\text{m}$  and from 224  $\mu\text{m}$  until 356  $\mu\text{m}$ . The developed model has 7 latent variables and accounts for high variance in both the X-data set (>99.9%) and the Y-data set (>85.6%). An external validation was performed using 25% of the available data set, which had not been used for calibration. Fig. 11 shows the experimental batch-level model scores versus model predictions.

These results show that there is a very good agreement between MRT and particle size of the final granules. The developed model is not intended to calibrate the MRT sensor for particle size, as it does not show enough accuracy and precision for that. Further improvement should be required, such as to increase the number of sam-

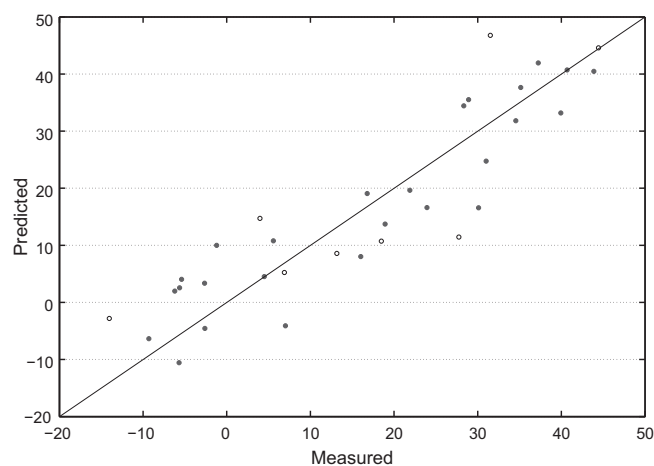


**Fig. 11.** PLS model: experimental versus predicted batch-level scores (full circles: calibration data set, open circles: external validation).  $R^2 = 0.810$ , RMSECV = 19.8, RMSEP = 10.2.

ples. However, it is possible to forecast approximately how much of the final granules will be within the ranges 12.6–20  $\mu\text{m}$  and 224–356  $\mu\text{m}$ , based on the MRT path of that run. In practice, for a given granulation trajectory, measured by MRT, the developed batch-level model can be applied, and a first principal component score will be generated. Through the iPLS model, this score can be translated into the fraction of the final granules that lie into the particle size ranges 12.6–20  $\mu\text{m}$  and 224–356  $\mu\text{m}$ . This unobvious new feature of the MRT sensor has a great potential, because time can now be saved in avoiding *off-line* particle size determinations. Moreover, the batch trajectory leading to a given targeted particle size distribution of the final granules can be followed and controlled. This allows, e.g., the process engineer or the operator to run the process in order to meet that target, achieving the QbD objectives.

## 4. Conclusions

A recent commercially available *in-line* MRT sensor that had previously been tested in a pharmaceutical environment small-scale fluid bed process [2] was now used in our study of a granula-



tion process at industrial scale. By analysing the MRT *in-line* measurements with MVDA, significant process knowledge regarding the granulation process was gained, using only historical process data and a few *off-line* particle size measurements.

The multivariate data analysis put into evidence a noticeable seasonality effect that influences the ongoing process as depending on the season of the year and leads to some differences on the final granule size histograms. A very good correlation between the MRT timely measurements (expressed as a batch-level model score) and the fraction of the final granules within two particular particle size ranges (12.6–20 µm and 224–356 µm) was achieved, through a PLS regression model. This highlights a new potential ability of the *in-line* microwave sensor to translate a granulation trajectory into particle size properties of the final granules.

It was shown that for a fluid bed dryer, process knowledge can be established, without disrupting or in any way affecting production and using process information that is already available. Only a few laboratory analyses were performed. This study follows PAT and QbD principles.

## Acknowledgements

The authors want to thank the following persons, all from Merck KGaA: Dr. Daniel von Bamberg and Mr. Jörg Wiese and his whole team for their overall support of the project; Dr. Jens Schewitz for carefully reviewing the manuscript; Dr. Reiner Vogt and Ms. Annette Hasse for the particle size measurements; Ms. Sandra Schreiner, Ms. Melanie Kowolik and Ms. Martina Lehrian for their kind and untiring help; Ms. Maria Leonor Alvarenga for the scientific discussions while preparing the manuscript.

## References

- [1] G. Singh, R. Sidwell, Sizing of granulation, in: D.M. Parikh (Ed.), Handbook of Pharmaceutical Granulation Technology, second ed., Informa Healthcare USA Inc., New York, 2007, pp. 491–533.
- [2] C. Buschmüller, W. Wiedey, C. Döscher, J. Dressler, J. Breitzkreutz, In-line monitoring of granule moisture in fluidized-bed dryers using microwave resonance technology, Eur. J. Pharm. Biopharm. 69 (2008) 380–387.
- [3] T. Schaefer, O. Worts, Control of fluidized bed granulation. III. Effects of inlet air temperature and liquid flow rate on granule size and size distribution. Control of moisture content of granules in the drying phase, Arch. Pharm. Chem. 6 (1978) 1–13.
- [4] P. Frake, D. Greenhalgh, S.M. Grierson, K.J.M. Hempenstall, D.R. Rudd, Process control and end-point determination of a fluid bed granulation by application of near infra-red spectroscopy, Int. J. Pharm. 151 (1997) 75–80.
- [5] J. Rantanen, E. Räsänen, J. Tenhunen, M. Käsäkoski, J. Mannermaa, J. Yliruusi, In-line moisture measurement during granulation with a four-wavelength near infrared sensor: an evaluation of particle size and binder effects, Eur. J. Pharm. Biopharm. 50 (2000) 271–276.
- [6] J. Rantanen, S. Lehtola, P. Rämetsä, J.P. Mannermaa, J. Yliruusi, On-line monitoring of moisture content in an instrumented fluidized bed granulator with a multi-channel NIR moisture sensor, Powder Technol. 99 (1998) 163–170.
- [7] Glatt GmbH, Method for monitoring and/or controlling and regulating a granulation, agglomeration, instantization, coating and drying process in a fluidized layer or a fluidized bed by determining product moisture, and device for carrying out said method, EP 0970369B1, 1997.
- [8] C. Döscher, W. Gähler, Mikrowellen-Resonatortechnik – Ein neues Prinzip zur Wassergehaltsbestimmung für die Zuckerindustrie, Zuckerindustrie 119 (1994) 375–378.
- [9] J. Döscher, Die Dichte ist egal, Process 11 (2002) S.44–45.
- [10] R. Knöchel, W. Taute, C. Döscher, Stray field ring resonators and a novel trough guide resonator for precise microwave moisture and density measurements, Meas. Sci. Technol. 18 (2007) S.1061–1068.
- [11] U. Klute, Microwave measuring technology for the sugar industry, Int. Sugar J. 109 (2007) 749–755.
- [12] K.-H. Theisen, I. Geyer, Microwave technology: an ubiquitous in line measurement instrument for density, total solids, concentration, especially brix in today's sugar factory, Int. Sugar J. 109 (2007) 310–319.
- [13] T. Jayanthi, B.S. Sreeja, G. Sundari, Moisture measurement in paper industry using microwave nondestructive method, in: Proceedings of the 6th International Conference on Measurement, Smolenice, Slovakia, 20–24, May 2007, pp. 241–246.
- [14] V.V. Lisovsky, Automatic control of moisture in agricultural products by methods of microwave aquametry, Meas. Sci. Technol. 18 (2005) 1016–1021.
- [15] L. Gradinarsky, H. Brage, B. Lagerholm, I.N. Björn, S. Folestad, In situ monitoring and control of moisture content in pharmaceutical powder processes using an open-ended coaxial probe, Meas. Sci. Technol. 17 (2006) 1847–1853.
- [16] T. Kourti, Process analytical technology beyond real-time analyzers: the role of multivariate analysis, Crit. Rev. Anal. Chem. 36 (2006) 257–278.
- [17] T. Kourti, The process analytical technology initiative and multivariate process analysis, monitoring and control, Anal. Bioanal. Chem. 384 (2006) 1043–1048.
- [18] T. Kourti, Abnormal situation detection, three-way data and projection methods; robust data archiving and modeling for industrial applications, Annu. Rev. Control 27 (2003) 131–139.
- [19] L. Erikson, E. Johansson, N. K.-Wold, J. Trygg, C. Wikström, S. Wold, Multi- and Megavariate Data Analysis – Part I. Basic Principles and Applications, second ed., Umetrics, Umea (Sweden), 2006.
- [20] L.X. Yu, Pharmaceutical quality by design: product and process development, understanding, and control, Pharm. Res. 25 (2006) 781–791.
- [21] S.S. Jambhekar, Bioavailability and granule properties, in: D.M. Parikh (Ed.), Handbook of Pharmaceutical Granulation Technology, second ed., Informa Healthcare, USA Inc., New York, 2007, pp. 535–543.
- [22] FDA, Process analytical technology initiative, guidance for industry PAT – a framework for innovative pharmaceutical development, manufacturing, and quality assurance, 2004. <<http://www.fda.gov/cmv/guidance/published.html>>.
- [23] ICH, Pharmaceutical Development – Q8, November 2004. <<https://www.ich.org/LOB/media/MEDIA4986.pdf>>.
- [24] ICH, Quality Risk Management – Q9, November 2005. <<http://www.ich.org/LOB/media/MEDIA1957.pdf>>.
- [25] <http://www.hydorpharm.com>.
- [26] A. Savitsky, H.J.E. Golay, Smoothing and differentiation of data by simplified least squares procedures, Anal. Chem. 36 (1964) 1627–1639.
- [27] A. Kassidas, J.F. MacGregor, P.A. Taylor, Synchronization of batch trajectories using dynamic time warping, AIChE J. 44 (1998) 864–875.
- [28] L. Norgaard, A. Saudland, J. Wagner, J.P. Nielsen, L. Munck, S.B. Engelsen, Interval partial least-squares regression (iPLS): a comparative chemometric study with an example from near-infrared spectroscopy, Appl. Spectrosc. 54 (2000) 413–419.
- [29] T. Lipsanen, Novel description of a design space for fluidised bed granulation, Int. J. Pharm. 345 (2007) 101–107.
- [30] D. Kunii, O. Levenspiel, Fluidization Engineering, second ed., Butterworth-Heinemann, New York, 1991.
- [31] F.J.S. Nieuwmeijer, K. van der Voort Maarschalk, H. Vromans, Granule breakage during drying processes, Int. J. Pharm. 329 (2006) 81–87.